




## Article

# Oral Administration of Platinum Nanoparticles with SOD/CAT Cascade Catalytic Activity to Alleviate Ulcerative Colitis

Hao Liu <sup>1,†</sup>, Yujie Zhang <sup>2,†</sup> , Mingzhen Zhang <sup>2</sup> , Zhaoxiang Yu <sup>3,\*</sup> and Mingxin Zhang <sup>4,\*</sup> 

<sup>1</sup> Second Clinical Medical College, Shaanxi University of Chinese Medicine, Xianyang 712046, China; 221030111836@sntcm.edu.cn

<sup>2</sup> School of Basic Medical Sciences, Xi'an Jiaotong University Health Science Center, Xi'an 710061, China; zhangyujie@xjtu.edu.cn (Y.Z.); mzhang21@xjtu.edu.cn (M.Z.)

<sup>3</sup> Department of General Surgery, The First Affiliated Hospital of Xi'an Medical University, Xi'an 710077, China

<sup>4</sup> Department of Gastroenterology, The First Affiliated Hospital of Xi'an Medical University, Xi'an 710077, China

\* Correspondence: zmx3115@xjtu.edu.cn (M.Z.); yuzhaoxiang@xjtu.edu.cn (Z.Y.)

† These authors contributed equally to this work.

**Abstract:** Ulcerative colitis (UC) is a refractory chronic inflammatory disease involving the colon and rectum, falling under the category of inflammatory bowel disease (IBD). The accumulation of reactive oxygen species (ROS) in local tissues has been identified as a crucial contributor to the escalation of inflammatory responses. Therefore, eliminating ROS in the inflamed colon is a promising approach to treating UC. Nanomaterials with intrinsic enzyme-like activities (nanozymes) have shown significant therapeutic potential in UC. In this study, we found that platinum nanoparticles (Pt NPs) exhibited remarkable superoxide dismutase (SOD) and catalase (CAT) cascade catalytic activities, as well as effective hydroxyl radical ( $\bullet\text{OH}$ ) scavenging ability. The *in vitro* experiments showed that Pt NPs could eliminate excessive ROS to protect cells against oxidative stress. In the colitis model, oral administration of Pt NPs (loaded in chitosan/alginate hydrogel) could significantly alleviate UC, including reducing the colon length, the damaged epithelium, and the infiltration of inflammatory cells. Without appreciable systemic toxicity, Pt NPs represent a novel therapeutic approach to UC and are expected to achieve long-term inflammatory remission.



**Citation:** Liu, H.; Zhang, Y.; Zhang, M.; Yu, Z.; Zhang, M. Oral Administration of Platinum Nanoparticles with SOD/CAT Cascade Catalytic Activity to Alleviate Ulcerative Colitis. *J. Funct. Biomater.* **2023**, *14*, 548. <https://doi.org/10.3390/jfb14110548>

Academic Editors: Alexander K. Andrianov and Nenad Ignjatovic

Received: 1 October 2023

Revised: 4 November 2023

Accepted: 13 November 2023

Published: 15 November 2023



**Copyright:** © 2023 by the authors. Licensee MDPI, Basel, Switzerland. This article is an open access article distributed under the terms and conditions of the Creative Commons Attribution (CC BY) license (<https://creativecommons.org/licenses/by/4.0/>).

**Keywords:** ulcerative colitis; platinum (Pt NPs); nanozymes; hydrogels; ROS scavenging

## 1. Introduction

Ulcerative colitis (UC), a chronic idiopathic inflammatory bowel disease (IBD), frequently results in sustained mucosal damage spanning from the rectum to the proximal colon [1,2]. Prolonged diarrhea, abdominal pain, recurrent bloody stool, and other symptoms significantly impact the daily life of individuals with UC. In recent decades, the prevalence of UC has surged in newly industrialized nations, particularly in East Asia [3–6]. While genetic and environmental factors are commonly implicated in the etiology of UC, the precise mechanisms underlying its pathogenesis remain elusive [7,8]. Combined treatment with chemical and biological agents such as 5-aminosalicylic acid (5-ASA), cortisol, and calcitonin inhibitors is the predominant approach to managing UC [9,10]. However, long-term, high-dose chemotherapy drugs frequently result in severe complications, including infection or thrombosis, necessitating surgical intervention for some UC patients due to complications such as intestinal stenosis or fistula [11–13]. Consequently, developing an innovative treatment for IBD is significant in addressing clinical challenges.

Prior research has demonstrated that a considerable quantity of inflammatory cells aggregate within the colon of individuals with inflammatory bowel disease (IBD), leading to the generation of reactive oxygen species (ROS), including hydrogen peroxide ( $\text{H}_2\text{O}_2$ ), hydroxyl radical ( $\bullet\text{OH}$ ), and superoxide anion ( $\text{O}_2\bullet^-$ ) [14,15]. The resultant oxidative stress caused by ROS instigates harm to the intestinal mucosa, thereby compromising

cellular structures such as the intestinal cell membrane, protein, and DNA, consequently exacerbating the advancement of IBD [16]. Therefore, using antioxidant enzymes to eliminate surplus ROS within the inflammatory microenvironment proves highly advantageous in upholding intestinal redox equilibrium and effectively managing UC [17]. Natural enzymes have high substrate specificity and catalytic activity. Still, their high cost and low stability have become the primary intrinsic defects that limit their wide application in the medical field [18,19].

In recent times, considerable scholarly focus has been directed toward artificial enzymes, which can imitate the functionality and specificity exhibited by natural enzymes. These artificial nanozymes offer a cost-effective alternative and address the inherent instability associated with natural enzymes. Consequently, they hold significant promise for application in disease diagnosis and treatment [20,21].

Platinum nanoparticles (Pt NPs) are emerging as a new class of nanozymes with distinct side effects and unique electronic structures, and these properties endow Pt NPs with potent superoxide dismutase (SOD) and catalase (CAT) activities, which can cascade catalyze  $O_2^{\bullet-}$  decomposition [22]. Previous studies have demonstrated the successful synthesis of Pt NPs (30 nm) as antioxidant agents for preventing and treating hepatic ischemia-reperfusion injury [23]. Moreover, Pt NPs have shown potential as antioxidant drugs for atherosclerosis by effectively eliminating the ROS produced by vascular endothelial cells under high glucose and lipid level conditions [24]. Therefore, the Pt-NP-based treatment of UC is a promising strategy for disease management.

Polyvinylpyrrolidone (PVP) is a kind of non-toxic, non-ionic polymer, and its unique chemical structure allows it to be used as a stabilizer to prevent the aggregation of nanoparticles in water or other organic solvents during the preparation of nanomaterials [25]. We considered the synthesis of Pt NPs using PVP. Chitosan/sodium alginate hydrogels, known for their excellent biocompatibility and biodegradability, are commonly used as carriers for nanomaterials [26,27]. Hydrogels enable drug delivery and sustained release within the gastrointestinal tract by loading anti-inflammatory or immunomodulatory drugs, enhancing therapeutic efficacy at inflammatory sites. It is worth mentioning that chitosan exhibits adhesive properties in the intestinal mucosa, further enhancing the drug concentration at sites of inflammation [28]. Therefore, selecting hydrogels for encapsulating Pt NPs holds promise for treating UC.

In this study, we synthesized Pt NPs with a reduced particle size to evaluate their therapeutic potential for UC. We mixed chloroplatinic acid hexahydrate ( $H_2PtCl_6 \cdot 6H_2O$ ) with PVP to prepare small-particle-size Pt NPs via reduction (Figure 1). To achieve targeted therapy and complete the construction of the nano-delivery system, we further loaded Pt NPs into a PH-responsive chitosan/alginate hydrogel. Upon oral administration, the hydrogel swells and ruptures in the alkaline environment of the colon, facilitating the release of Pt NPs. The internalized Pt NPs effectively eliminate ROS at the inflamed sites within colonic epithelial cells, thereby preventing oxidative damage to the intestinal epithelium. The oral administration of Pt NPs loaded within the chitosan/alginate hydrogel offers a novel strategy for alleviating UC inflammation.

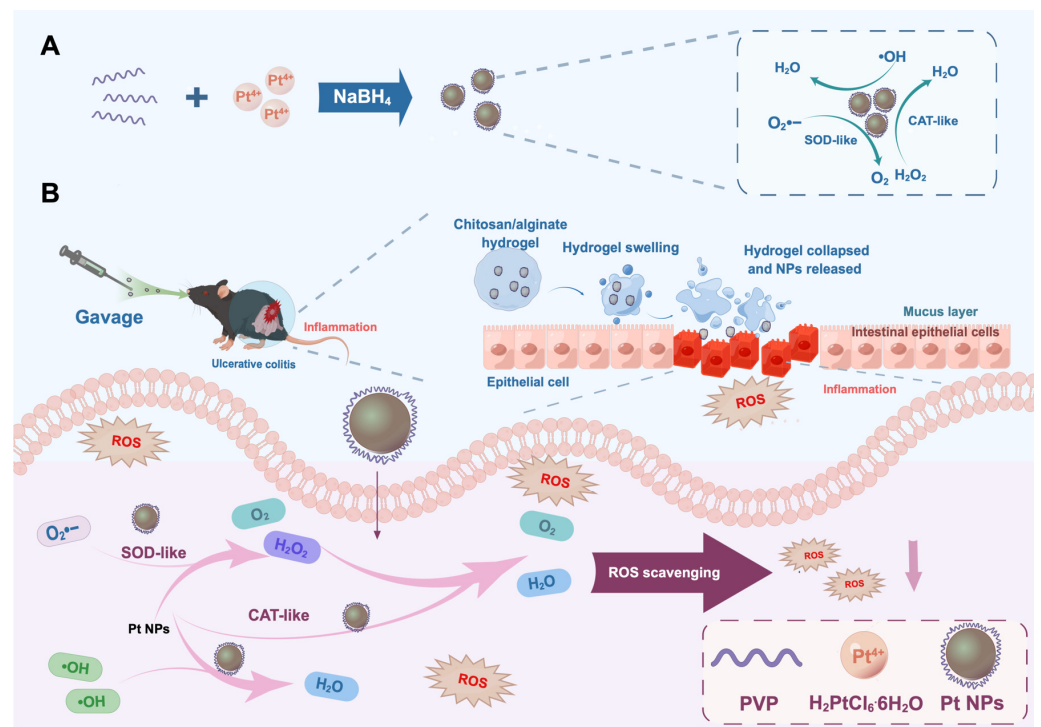


**Figure 1.** Schematic of the synthesis of Pt NP nanozymes and oral administration of Pt NPs encapsulated in chitosan/sodium alginate hydrogel to alleviate ulcerative colitis. (A) Synthesis of Pt NPs with enhanced SOD and CAT activities and •OH scavenging capacity via reduction method. (B) Oral administration of Pt NPs encapsulated in chitosan/sodium alginate hydrogel to alleviate ulcerative colitis.

## 2. Materials and Methods

### 2.1. Materials and Instruments

The chloroplatinic acid hexahydrate ( $\text{H}_2\text{PtCl}_6 \cdot 6\text{H}_2\text{O}$ ), terephthalic acid (TA), and polyvinylpyrrolidone (PVP) were purchased from Aladdin Technology Co., Ltd. (Shanghai, China). The sodium borohydride ( $\text{NaBH}_4$ ) was obtained from Sinopharm Group Chemical Reagent Co., Ltd. (Shanghai, China). The nitroblue tetrazolium chloride (NBT), L-methionine (L-met), and riboflavin were all sourced from Sigma-Aldrich (Shanghai, China). The hydrogen peroxide ( $\text{H}_2\text{O}_2$ , 30%) was obtained from Beijing Chemical Reagents Company (Tianjin, China). The methylene blue (MB) was purchased from Chemical Reagent Co., Ltd. (Tianjin, China). The ferrous chloride dihydrate ( $\text{FeCl}_2 \cdot 4\text{H}_2\text{O}$ ) was acquired from Bioren Biological Technology Co., Ltd. (Tianjin, China). The 2,7-dichlorofluorescein diacetate (DCFH-DA) was sourced from Beyotime Biotechnology (Shanghai, China). The chitosan was acquired from Tokyo Chemical Industry Co, Ltd. (Tokyo, Japan), the sodium alginate from Aladdin Co, Ltd. (Shanghai, China), and the 5-aminosalicylic acid (5-ASA) from Sangon Biotech Co., Ltd. (Shanghai, China).

The primary experimental equipment utilized in the study included a transmission electron microscope (JEOL JEM-2100Plus, Tokyo, Japan), X-ray diffractometer (Bruker D8 ADVANCE, Bruker, Billerica, MA, USA), ultraviolet absorption spectrophotometer (UV-2700, Shimadzu Corporation, Kyoto, Japan), Malvern particle size analyzer (Nano ZSE, Malvern, Shanghai, China), dissolved oxygen meter (JPSJ-605F, Leybold, Shanghai, China), and fluorescence spectrophotometer (Hitachi F-4700, Hitachi, Tokyo, Japan).

### 2.2. Preparation and Characterization of Pt NPs

The Pt nanoparticles were synthesized via chemical reduction. Respectively, 86 mg of PVP and 27.13 mg of  $\text{H}_2\text{PtCl}_6 \cdot 6\text{H}_2\text{O}$  were dissolved in 51.4 mL and 8.6 mL of water. The two solutions were mixed. Subsequently, 1 mL of  $\text{NaBH}_4$  solution (10 mg/mL) was

added dropwise under continuous stirring. The solution exhibited a color change from yellow to dark brown and generated many bubbles. After completion of stirring, the solution was allowed to stand undisturbed for 24 h, followed by rotary evaporation for 15 min to reduce the solution volume. Water dialysis was conducted for 24 h to remove the  $\text{NaBH}_4$  residues, followed by subsequent rotary evaporation to obtain a precipitate of the Pt colloid. The deposit was then treated with 3 mL of acetone and subjected to sonication, after which rotary evaporation was applied to remove the residual acetone. A volume of 2 mL of ethanol was introduced into the sediment and subjected to sonication for a duration (15 min). The resulting mixture was blended and subsequently subjected to centrifugation (3000 rpm/10 min). The washing process was repeated three times using ethanol and hexane to ensure the removal of excess PVP. Finally, the Pt NPs synthesis was concluded by resuspending the residue in 2 mL of water.

The total Pt content in the aqueous Pt NPs was determined using inductively coupled plasma atomic emission spectrometry (ICP-AES). The morphology and size of the Pt NPs were characterized using transmission electron microscopy (TEM). X-ray diffraction (XRD) analysis was utilized to ascertain the crystal structure of the Pt nanoparticles. The optical properties of Pt NPs were evaluated by measuring the ultraviolet-visible (UV-Vis) spectra using an ultraviolet absorption spectrophotometer. The stability of the Pt NPs was assessed by measuring their zeta potential using a Malvern ZS90 particle size analyzer.

### 2.3. SOD-like Activity of Pt NPs

The SOD-like activity of the Pt NPs was tested using the NBT reduction method. Riboflavin undergoes reduction when exposed to light, followed by subsequent oxidation in the presence of oxygen to generate  $\text{O}_2^{\bullet-}$ . This reactive oxygen species then reacts with NBT to form a blue methyl hydrazone compound, which exhibits its maximum absorption at 560 nm. The nanoparticles (NPs) possessing superoxide dismutase (SOD) activity effectively scavenge  $\text{O}_2^{\bullet-}$ , thereby inhibiting the formation of methyl hydrazone. The experimental setup constructed a reaction system by mixing L-MET (13 mM), riboflavin (20  $\mu\text{M}$ ), NBT, and PBS buffer. Subsequently, Pt NPs with varying concentrations (0–100  $\mu\text{g}/\text{mL}$ ) were added. Following continuous illumination for 2 min, the absorption at 560 nm was quantified using a microplate reader.

### 2.4. CAT-like Activity of Pt NPs

The CAT activity of the Pt NPs was measured using the dissolved oxygen method. CAT enzyme catalyzes the decomposition of  $\text{H}_2\text{O}_2$  to produce oxygen. Different concentrations (0.1, 0.2, 0.4, 0.8, 1, 1.5  $\mu\text{g}/\text{mL}$ ) of Pt NPs were added to a 10 mL ultrapure water system containing the same concentration of  $\text{H}_2\text{O}_2$ . The dissolved oxygen meter was adjusted to the kinetic mode to monitor the changes in oxygen content (mg/L) in the reaction solution. Using the same method, equal amounts of Pt NPs were introduced into a 10 mL ultrapure water system containing different concentrations of  $\text{H}_2\text{O}_2$  (200  $\mu\text{M}$ , 1 mM, and 2 mM) to study the substrate concentration dependence of the CAT enzyme activity of the Pt NPs.

Michaelis–Menten constant determination was performed by setting up different concentrations of  $\text{H}_2\text{O}_2$  (0.5, 1, 2, 4, 8, 16, 32, 64, 96, 128, and 144 mM) in a 10 mL ultrapure water reaction system. An equal amount of Pt NPs with a concentration of 0.175  $\mu\text{g}/\text{mL}$  was added to the system. The oxygen concentration (mg/L) was subsequently measured using a dissolved oxygen meter, and the measurements were concluded once the oxygen concentration reached equilibrium.

### 2.5. $\bullet\text{OH}$ Scavenging Capacity Test

We validated the  $\bullet\text{OH}$  scavenging ability of aqueous solutions of Pt NPs using two methods.

Method One: Methylene blue (MB) fading strategy. The absorption peak of MB in the visible range is at 664 nm. The  $\bullet\text{OH}$  generated by Fenton's reagent can cause the fading of MB, leading to a reduction in its absorption at 664 nm. Pt NPs at a concentration of

25 µg/mL were mixed with 1 mM Fe<sup>2+</sup> and 5 mM H<sub>2</sub>O<sub>2</sub> in PBS buffer (25 mM, pH 7.4), and the mixture was incubated at 37 °C for 15 min. Subsequently, 0.25 mM MB was added, and the absorbance of MB at 664 nm was measured using a UV spectrophotometer.

Method Two: Terephthalic acid (TA) method. Ultraviolet (UV) radiation can induce the production of a large amount of •OH from H<sub>2</sub>O<sub>2</sub>, and •OH readily reacts with TA to form 2-hydroxyterphenylacid, which exhibits fluorescence properties (excitation wavelength: 320 nm, emission wavelength: 425 nm). After irradiation of the PBS buffer containing H<sub>2</sub>O<sub>2</sub> (5 mM) and TA (0.5 mM) under UV light for 15 min, different concentrations of Pt NPs (12.5, 25, 50, 100 µg/mL) were added, and the fluorescence intensity of the mixture was measured using a fluorescence spectrophotometer.

#### 2.6. Anti-Oxidative Effect of Pt NPs in Living Cells

The RAW 264.7 cells were purchased from Procell Co., Ltd (Wuhan, China). The RAW 264.7 cells were evenly distributed in 6-well plates at  $5 \times 10^3$  cells/well density and incubated overnight at 37 °C. The Pt NP solution (50 µg/mL) was prepared using Dulbecco's Modified Eagle's Medium (DMEM) and incubated for an additional 8 h. The medium was removed, and the cells were treated with a solution of a ROS-positive control, named Rosup (0.5 mg/mL), for 30 min to induce the production of ROS. The cells were stained using 10 µM of 2, 7-dichlorofluorescein diacetate (DCFH-DA) and examined using a fluorescence microscope.

#### 2.7. Preparation of Chitosan/Alginate Hydrogel

The chitosan/alginate saline gel was prepared according to the relevant literature [29–31]. Chitosan powder was dissolved in acetic acid, and the pH was adjusted to approximately 7.0 using a NaOH solution (0.15 mol·L<sup>-1</sup>). The resulting solution was then scaled to a final concentration of 0.6% (wt./vol) and stirred overnight at room temperature. Sodium alginate was dissolved in a 0.15 M NaCl solution, and the final concentration was adjusted to 1.4% (wt./vol). The chitosan and sodium alginate solutions were mixed in a 1:1 ratio, and the nanoparticles were added. The chelating solution, containing 30 mM Na<sub>2</sub>SO<sub>4</sub> and 140 mM CaCl<sub>2</sub>, was prepared at a 1:1 volume ratio. Before utilization, the polysaccharide solution and the chelating solution containing the nanoparticles underwent preheating at 37 °C for 30 min.

#### 2.8. Animals

The present study was approved by the Animal Ethics Committee of Xi'an Jiaotong University (ethical protocol approval n. XJTUAE2023-1564). Female C57/BL6 mice (8 weeks old) were obtained from the Animal Center of Xi'an Jiaotong University Health Science Center, Shaanxi province, China. The mice were housed under standard laboratory conditions, following the animal care and use guidelines.

#### 2.9. Colitis Model of Mice

Eight-week-old female C57 mice were randomly assigned to one of four groups: a healthy group, a DSS group, a DSS + 5-ASA group, and a DSS + Pt NPs group. Except for the healthy group, all mice received ad libitum administration of 2.5% w/v dextran sulfate sodium (DSS; 36–50 Kda) solution for seven days to induce acute UC. Throughout the modeling period, the mice in the treatment groups received gavage treatment on the 2nd, 4th, and 6th day. Daily weight changes, hematochezia, and disease activity index records were kept. On the 8th day, all mice were euthanized, and their distal colon tissues were collected for subsequent analysis.

#### 2.10. Statistical Analysis

The results were analyzed using a one-way ANOVA test and Student's *t*-test. Statistical significance: \*  $p < 0.05$ , \*\*  $p < 0.01$ , \*\*\*  $p < 0.001$ .

### 3. Results

#### 3.1. Synthesis and Characterization of Pt NPs

Firstly, the Pt NPs were synthesized using a reduction method [32]. The morphology of the prepared Pt NPs was observed using TEM, revealing a uniform and stable distribution in the aqueous solution (Figure 2A) [33]. The size distribution histogram of the Pt NPs, mounted using the Sturges method, revealed an average particle diameter size of  $3 \pm 1$  nm (Figure 2B) [34]. The XRD technique was employed to determine the crystal structure of Pt NPs. The results illustrated the distinct diffraction peaks observed at  $2\theta$  values of  $39.9^\circ$ ,  $46.1^\circ$ ,  $68.1^\circ$ , and  $81.5^\circ$ , which corresponded to the 111, 200, 220, and 311 planes of the Pt crystal morphology, respectively (Figure 2C). All these results provided evidence for the successful synthesis of the Pt NPs.

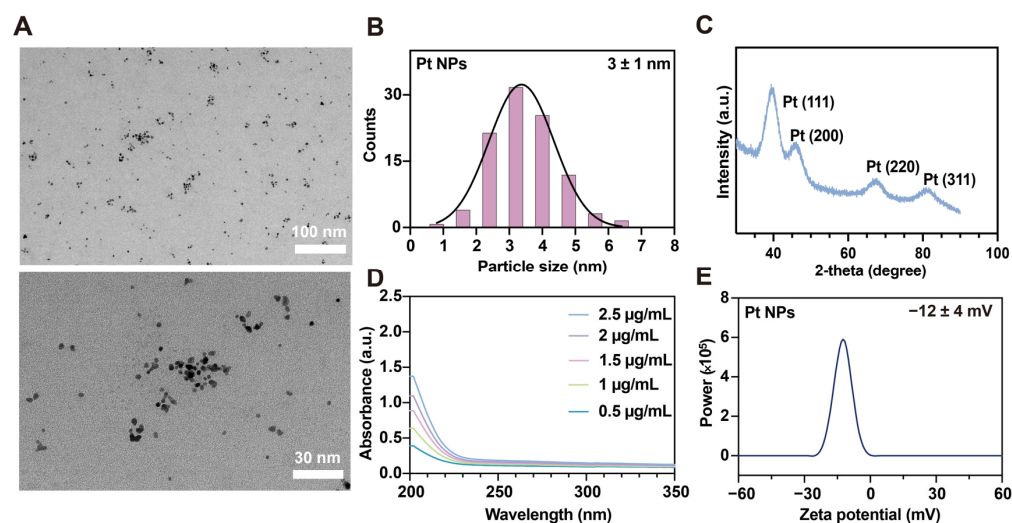


**Figure 2.** Characterization studies of Pt NPs. (A) TEM images of Pt NPs. Scale bar: 100 nm; 30 nm. (B) Particle size distribution of Pt NPs.  $N = 126$ . The solid black line represents the fitted distribution function:  $Y = 32.32 \times \exp(-0.5 \times ((X - 3.369)/0.9812)^2)$ . (C) X-ray powder diffraction pattern of Pt NPs. (D) UV-vis absorption spectra of Pt NPs with different concentrations. (E) Zeta potential of Pt NPs.

The presence of an absorption peak in the  $H_2PtCl_6$  solution is attributed to the  $PtCl_6^{2-}$  ions. In specific sizes and shapes, such as nanoscale surface coatings, platinum nanoparticles exhibit a visible absorption peak within the UV spectrum due to the surface plasmon resonance effect. However, conventional platinum nanoparticle colloidal solutions usually lack absorption peaks in the UV spectrum range. This study's UV-visible spectroscopic analysis of Pt NPs with varying concentrations confirmed the absence of absorption peaks within the UV spectrum range, consistent with previous research findings (Figure 2D) [35–37]. Colitis frequently results in mucosal layer impairment, causing an accumulation of positively charged molecules in the affected epithelial region. Consequently, negatively charged nanomaterials have the potential to explicitly target and treat inflamed epithelia [38]. The zeta potential technique serves as an indirect means of assessing the surface charge of nanoparticles. The stability of Pt NPs was evaluated by measuring the zeta potential [39]. The results reveal that the zeta potential of Pt NPs in an aqueous solution was  $-12 \pm 4$  mV (Figure 2E). The characteristic negative charge promisingly facilitated the rapid targeting of Pt NPs to sites of inflammation, thereby enhancing the therapeutic effectiveness.

#### 3.2. ROS Scavenging Ability of the Pt NPs

The antioxidant capabilities of nanomaterials are crucial for an anti-inflammatory therapeutic role. Hence, the antioxidant activity of the Pt NPs was further evaluated. The NBT method was utilized to examine the SOD-like activity of the Pt NPs. The results revealed that the SOD activity of the Pt NPs increased with rising concentrations, and the

Pt NPs eliminated  $O_2^{\bullet-}$  at a concentration of 100  $\mu\text{g}/\text{mL}$  (Figure 3A). The SOD enzyme facilitates the dismutation of  $O_2^{\bullet-}$  to generate  $H_2O_2$ , which possesses oxidizing properties, and the CAT enzyme can catalyze  $H_2O_2$  into non-toxic oxygen and water. The dissolved oxygen method was employed to measure the CAT-like enzyme activity of the Pt NPs. The findings indicated that Pt NPs exhibited significant efficacy in catalyzing oxygen production from  $H_2O_2$ . At room temperature, as the concentration of Pt NPs increased, the volume of oxygen produced also escalated (Figure 3B). Moreover, under the equivalent concentration of Pt NPs and varying concentrations of  $H_2O_2$ , Pt NPs exhibited substrate-concentration-dependent CAT-like enzyme activity (Figure 3C). The Michaelis–Menten kinetics were calculated, and it was determined that the  $K_M$  of Pt NPs was  $(37 \pm 2) \times 10^{-3} \text{ M}$  and the  $V_{max}$  was  $(55 \pm 1) \times 10^{-8} \text{ M}\cdot\text{min}^{-1}$ , which suggested that the Pt NPs demonstrated a good affinity for  $H_2O_2$  (Figure 3D).  $\bullet\text{OH}$  is another highly reactive oxidative ROS, and excessive  $\bullet\text{OH}$  in human cells often inflicts severe oxidative damage on the DNA structure [40]. To assess the efficacy of Pt NPs in eliminating  $\bullet\text{OH}$ , MB was employed as an indicator to detect  $\bullet\text{OH}$ . The methylene blue (MB) solution is blue, with an absorption peak at 664 nm in the visible range. The  $\bullet\text{OH}$  generated by Fenton's reagent causes the bleaching of the MB solution, resulting in a decrease in its absorption peak at 664 nm. The results showed that a single MB solution exhibited a distinct absorption peak at 664 nm, and the solution appeared blue. Introducing Fenton's reagent lightened the MB solution color and nearly eradicated the absorption peak at 660 nm. However, when Pt NPs were added to the mixture, the absorption peak at 660 nm was restored, indicating that Pt NPs can effectively eliminate  $\bullet\text{OH}$  (Figure 3E). Furthermore, the efficacy of the Pt NPs in eliminating  $\bullet\text{OH}$  was indirectly assessed by employing terephthalic acid (TA). Ultraviolet (UV) radiation can induce the production of a large amount of  $\bullet\text{OH}$  from  $H_2O_2$ , and  $\bullet\text{OH}$  readily reacts with TA to form 2-hydroxyterphenylacid, which exhibits fluorescence properties (excitation wavelength: 320 nm; emission wavelength: 425 nm). The experimental findings showed that the UV-irradiated TA mixture had an absorption peak at 425 nm, while the absorption peak of the TA mixture diminished after adding Pt NPs (Figure 3F). In addition, the extent of reduction in the absorption peak is proportional to the concentration of Pt NPs (Figure 3F). The observation suggested that Pt NPs eliminated the  $\bullet\text{OH}$  production and thus reduced the production of the fluorescent compound 2-hydroxyterphenylacid.

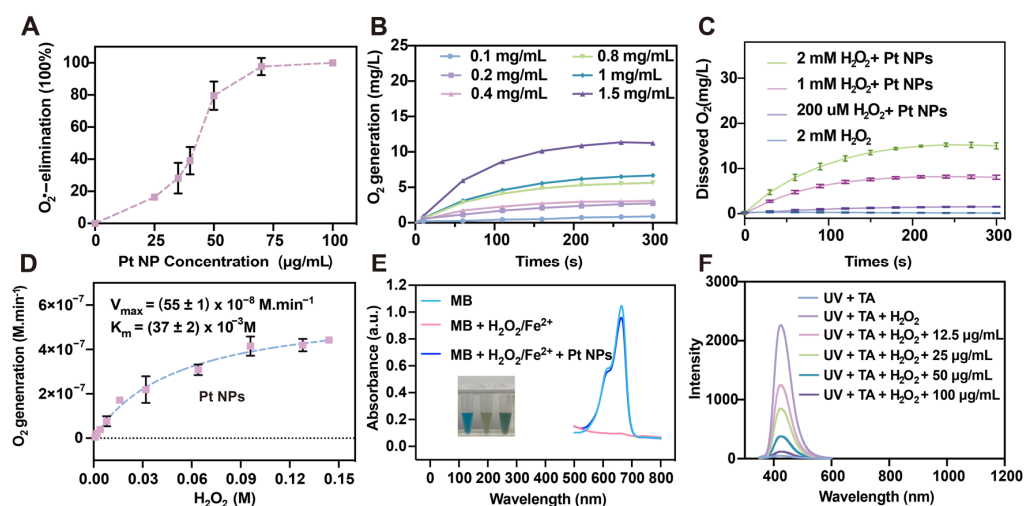


**Figure 3.** ROS scavenging capacity of the Pt NPs. (A) Percentage of  $O_2^{\bullet-}$  elimination by Pt NPs in various concentrations via the NBT method. (B) Dissolved oxygen production from  $H_2O_2$  under different Pt NP concentrations. (C) CAT-like enzyme activity of Pt NPs (1.75  $\mu\text{g}/\text{mL}$ ) under varied  $H_2O_2$  concentrations. (D) The Michaelis–Menten kinetics assay for the CAT-like enzyme activity of the Pt NPs (with 0.175  $\mu\text{g}/\text{mL}$  Pt NPs and 0–0.144 M  $H_2O_2$ ). (E) MB method determined the  $\bullet\text{OH}$  scavenging ability of the Pt NPs (20  $\mu\text{g}/\text{mL}$ ). Inset: Images of different reaction systems. (F) TA method determined the  $\bullet\text{OH}$  scavenging ability of the Pt NPs.

### 3.3. The Intracellular ROS Scavenging Capacity of Pt NPs

The large amount of ROS in the intestinal epithelial cells of IBD patients is closely related to the aggregation and activation of inflammatory cells (such as neutrophils) in the inflammatory site. The synergistic effect of the ROS and inflammatory cells leads to cell damage and oxidative stress, ultimately worsening the inflammatory microenvironment and exacerbating colitis symptoms [41]. Consequently, the elimination of excessive ROS within cells holds immense importance in the management of UC. The antioxidant potential of Pt NPs was examined at the cellular level. As a fluorescent probe, 2', 7'-dichlorofluorescein diacetate (DCFH-DA) was employed to detect intracellular ROS. DCFH-DA possesses the ability to permeate the cell membrane and react with intracellular ROS, resulting in the production of 2', 7'-dichlorofluorescein (DCF) with green fluorescence emission. By measuring the fluorescence intensity, the level of intracellular ROS could be indirectly evaluated [42]. Rosup was an exogenous inducer to elicit ROS in RAW 264.7 cells (macrophages typical in inflammatory responses), with a DCFH-DA probe for measuring the intracellular ROS levels. The results indicated that the control group and the group treated with Pt NPs exhibited negligible fluorescence in the RAW 264.7 cells, meaning that the cells had almost no ROS. The fluorescence intensity significantly increased in the cell group stimulated using Rosup, and after co-incubating with Pt NPs, a notable decrease in green fluorescence was observed, suggesting that Rosup effectively induced ROS production, and Pt NPs significantly reduced ROS. (Figure 4A). The conclusion was confirmed via statistical analysis of the fluorescence intensity (Figure 4B).

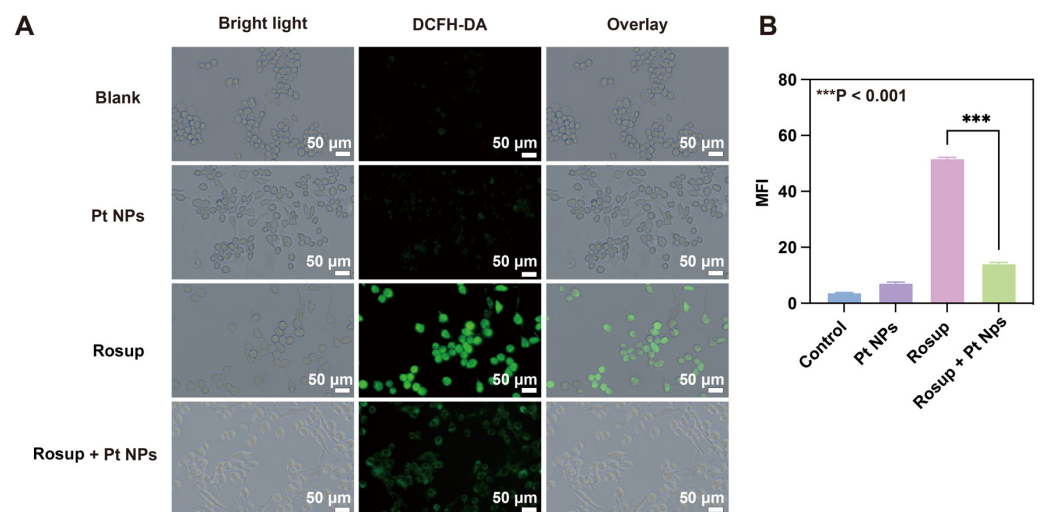


**Figure 4.** In vitro anti-oxidative of Pt NPs. (A) Characteristic fluorescence images of RAW 264.7 cells stained using DCFH-DA after various treatments. Scale bar: 50  $\mu\text{m}$ . (B) Mean fluorescence intensity of RAW 264.7 cells stained using DCFH-DA. \*\*\*  $p < 0.001$ .

### 3.4. In Vivo Determination of the Biocompatibility of Pt NPs

Nanomaterials used in biomedicine come into direct contact with blood and tissues when introduced into the human body, potentially causing toxic side effects [43,44]. Consequently, an animal experiment was devised to assess the biocompatibility of Pt NPs. A cohort of healthy mice was randomly allocated into two groups, wherein the treatment group was administered Pt NPs every alternate consecutive duration of 7 days. After 14 days, the mice were euthanized, and their organs and various gastrointestinal tract segments were collected for histological examination using hematoxylin and eosin staining. Blood samples were obtained from both groups of mice for biochemistry analysis and complete blood cell count (CBC). A comparison of the H and E staining results of the vital organs between the control and treatment groups did not reveal any significant differences, indicating no observable tissue damage in either group (Figure 5A). Specifically, the liver displayed a typical arrangement of hepatocytes without any evidence of necrotic edema.



The heart exhibited intact myocardial fibers and no cellular vacuolation. The histological analysis of the gastrointestinal tract tissues (including the stomach, duodenum, jejunum, ileum, and colon) obtained from mice treated using Pt NPs demonstrated comparable tissue morphology to the control group. No evidence of intestinal epithelial detachment, defects, or the infiltration of inflammatory cells was observed in either group (Figure 5B). The blood biochemical indexes of mice in both the administration group and the healthy group were assessed, encompassing alanine aminotransferase (ALT), aspartate aminotransferase (AST), creatinine (CREA), urea, creatine kinase (CK), and lactate dehydrogenase-1 (LDH-1). The findings indicated that all biochemical indexes in both groups were within the established normal range (Figure 5C).

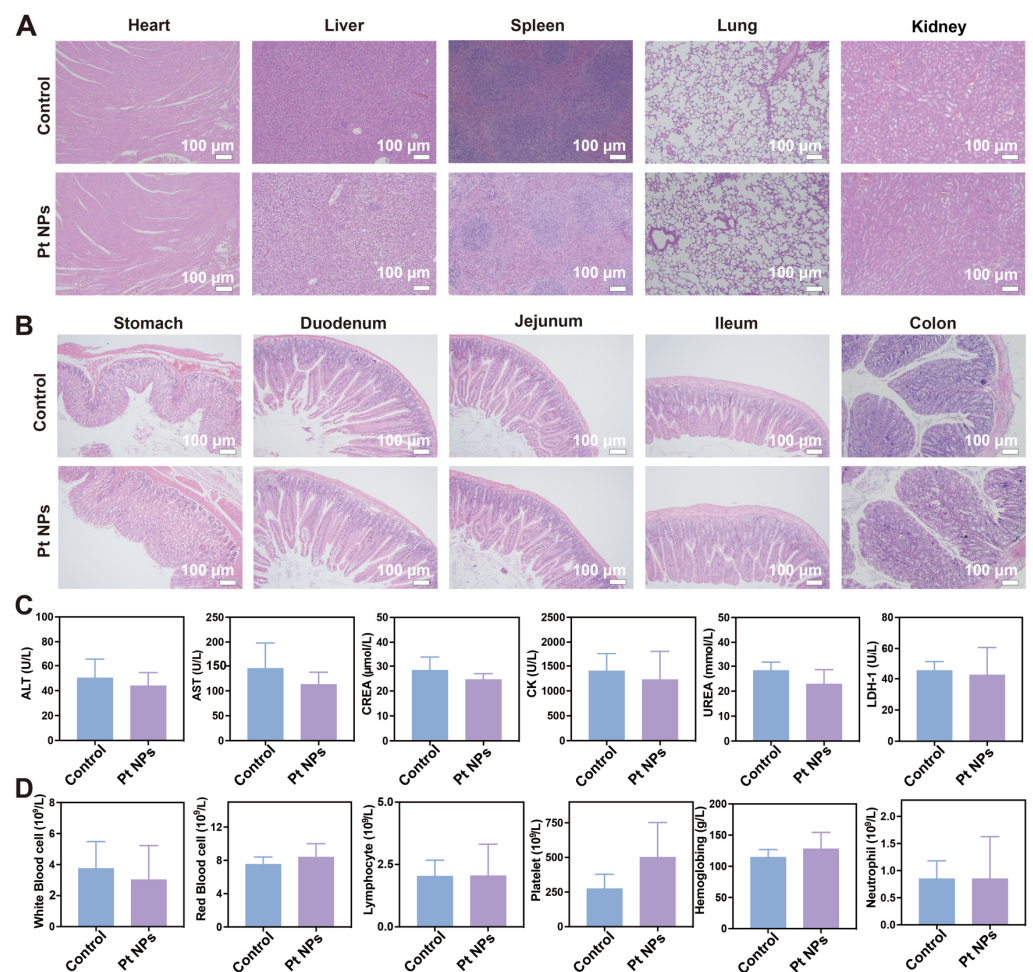


**Figure 5.** Biocompatibility evaluation of Pt NPs. (A) Histological assessment of major organs using HE staining to examine the systemic toxicity of Pt NPs. Scale bar: 100  $\mu$ m. (B) HE staining evaluation of Pt NP toxicity in the digestive system. Scale bar: 100  $\mu$ m. (C) Analysis of complete blood cell counts in mice treated using Pt NPs. (D) Analysis of blood biochemistry parameters in mice treated using Pt NPs.

Consequently, it could be inferred that Pt NPs did not induce significant harm to vital organs such as the liver, kidneys, and cardiac muscle in mice. CBC analysis showed no significant changes in the red blood cells, white blood cells, neutrophils, lymphocytes, platelets, and hemoglobin levels between the treatment group and the control group (Figure 5D). Consequently, based on these experimental findings, it can be inferred that orally administered chitosan/alginate-coated Pt NPs demonstrate favorable biocompatibility.

### 3.5. Protective Effect of Pt NPs against Colitis

The protective effect of Pt NPs on the colon was investigated in a UC mouse model induced by dextran sodium sulfate (DSS). Oral administration is preferred for ulcerative colitis treatment due to its simplicity, convenience, and safety [45]. The Pt NPs were encapsulated within a hydrogel composed of chitosan and sodium alginate for oral administration (Figure 6A, i). The hydrogel exhibited a tight structure in the gastric acid environment, preventing premature release of the Pt NPs. Nevertheless, upon arrival at the location of colonic inflammation, the alkaline surroundings prompted an escalation in the swelling characteristics of chitosan, resulting in the expansion of the hydrogel and subsequent liberation of the Pt NPs. The methodology accomplished targeted treatment of colonic inflammation via Pt NPs [46]. A 2.5% DSS solution was employed over 8 days to simulate acute UC in mice (Figure 6A, ii). In the treatment group, dosing was administered on days 2, 4, and 6. To evaluate the efficacy of the Pt NPs, 5-aminosalicylic acid (5-ASA) was employed as a positive control for treating UC. The body weight of the mice in different groups was monitored during the modeling and treatment period, reflecting the effects of modeling and treatment. The findings indicated that compared to the healthy group, mice subjected to DSS induction experienced weight reduction from day 5 (Figure 6B).

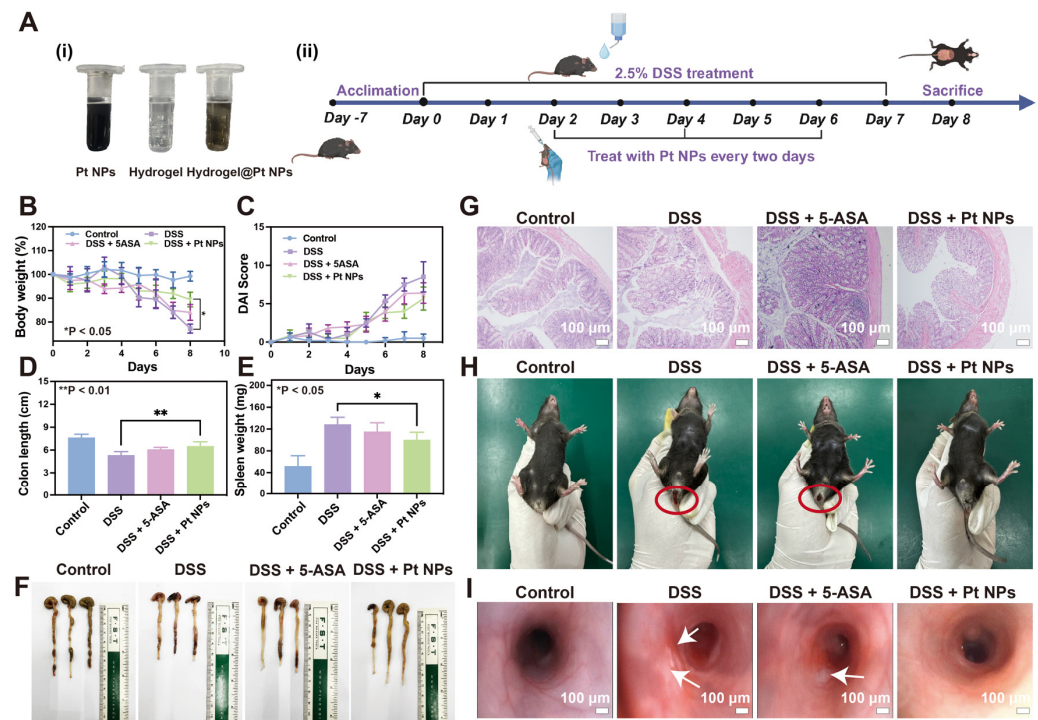


**Figure 6.** Protective effect of Pt NPs in the DSS-induced colitis model. (A) Diagram illustrating the application of Pt NPs in the treatment of DSS-induced colitis mice. (B) Weight changes in mice over 8 days. (C) Changes in DAI scores of mice over 8 days. (D) Assessment of colon length in mice subjected to different treatments. (E) Assessment of spleen weight in mice subjected to different treatments. (F) Photographs of excised colons from mice in different treatment groups showing differences in length. (G) HE-stained histological analysis of colonic tissues from mice subjected to different treatments on day 8. Scale bar: 100  $\mu$ m. (H) Representative photographs of rectal bleeding in the different groups. (I) Endoscopic images of the colon in the different groups. Scale bar: 100  $\mu$ m. \*  $p < 0.05$ , \*\*  $p < 0.01$ .

Meanwhile, mice treated with oral 5-ASA and Pt NPs showed a significantly milder decrease in body weight (Figure 6B). Furthermore, mice treated with Pt NPs exhibited a significantly lower disease activity index (DAI) than the DSS group (Figure 6C). As a vital immune organ, the weight change in the spleen can be used as an index to evaluate the level of inflammation [47]. The spleen of the mice was weighed after execution. The spleen

weight of the mice treated with Pt NPs was significantly lower than that of the DSS group, indicating effective prevention of inflammation by Pt NPs (Figure 6D). The colon length of mice induced using DSS was significantly reduced compared with that of healthy mice, while adding Pt NPs impeded this reduction in colon length (Figure 6E,F). Subsequently, the colon tissues of the mice were stained using hematoxylin–eosin (Figure 6E,H). The results showed the integrity of the colon epithelial cells in mice induced using DSS was destroyed, and many inflammatory cells infiltrated the intestinal epithelium, which was evidence of the inflammatory response, leading to cell damage and death [48]. The colonic continuity of mice with 5-ASA and Pt NP treatment remained largely intact, had no apparent instances of rupture, and exhibited a notable reduction in the infiltration of inflammatory cells (Figure 6G). Anal bleeding is a manifestation of extensive damage to the intestinal mucosa. During treatment, blood in the stool was observed in mice, particularly those with induced UC via DSS administration. However, mice treated with oral Pt NPs exhibited a reduction in the symptoms of anal bleeding (Figure 6H). Endoscopy is the preferred method for clinically diagnosing UC, offering precise lesion localization and evaluation of disease activity.

Moreover, it plays a crucial role in guiding the modification and implementation of treatment strategies for intestinal diseases [49,50]. The endoscopic results demonstrated that Pt NP treatment significantly reduced colon mucosal congestion, edema, and ulceration in the UC mouse model (Figure 6I). These results all supported that Pt NPs effectively prevent colitis.

#### 4. Discussion

UC has historically been characterized as a chronic inflammatory disorder resulting from an aberrant immune response. As the main symptoms of UC, recurrent bloody stool and diarrhea seriously affect the average life of patients [51]. Prolonged exposure to inflammatory factors can exacerbate colonic mucosal damage in certain UC patients, frequently leading to the development of inflammatory colon cancer [52,53]. In the clinical management of UC, the primary approach to achieving remission involves the utilization of 5-ASA and certain small molecular biological agents [54]. Nevertheless, administering these medications frequently results in severe infections or drug resistance among patients, ultimately heightening the likelihood of colectomy [55]. The excessive expression of immune cells, including neutrophils, in the colonic mucosa has been observed to promote the generation of abundant ROS and contribute to oxidative stress. The detrimental feedback loop between ROS and inflammatory responses is a primary driver of the rapid deterioration of UC. Thus, the utilization of antioxidant therapy represents a promising approach to the treatment of UC [56].

Traditional natural enzymes possess a commendable level of safety and exhibit remarkable catalytic activity, rendering them highly suitable for the therapeutic management of inflammation [57]. To illustrate, the extraction of polyphenolic compounds from *Nitraria tangutorum* Bobr. fruits had been undertaken by researchers to address colitis, and the efficacy of Manganese Superoxide Dismutase (Mn-SOD) treatment of UC had been substantiated via intramuscular administration in a mouse model of colitis [58,59]. However, there are technical limitations concerning the purification and extraction of natural enzymes, resulting in low purity and a complex purification process. Furthermore, since colitis is an inflammation of the gastrointestinal tract, oral administration is the preferred delivery route. Unfortunately, due to the protein nature of enzymes like SOD, their oral administration often leads to rapid degradation.

Consequently, muscle injection is frequently required, resulting in a shorter half-life and reduced efficacy of the therapeutic agents. Artificial nanoenzymes with efficient catalytic activity have been extensively studied as a new therapeutic approach to overcome the limitations and deficiencies of natural enzymes. Therefore, synthesizing a nanoenzyme drug that can efficiently and selectively combat oxidative damage at the inflamed sites in the colon holds significant value for treating UC [60].

In recent years, there has been growing recognition of the significant potential of Pt NPs in biomedical applications [61,62]. Previous research has provided evidence that Pt NPs, particularly those with smaller particle sizes, exhibit diverse antioxidant enzyme activities due to their distinctive electronic structure and size-dependent effects. These inherent properties render Pt NPs a promising and dependable novel material for addressing refractory inflammatory diseases that arise from the accumulation of ROS. Pt NPs are effective in treating neuroinflammatory conditions [63]. Due to their diminutive dimensions and reduced fluidity, nanogels demonstrate a limited capacity for drug encapsulation and inadequate durability as oral drug carriers, and the residual surfactants or unreacted monomers after nanogel preparation can head to toxic effects [64,65].

Nevertheless, many preliminary inquiries have provided evidence for the praiseworthy compatibility with living organisms and the ability to decompose naturally of chitosan/sodium alginate hydrogels. These hydrogels possess a permeable framework and expansive surface area, facilitating efficient adsorption and sustained retention of medicinal compounds. The commendable biocompatibility and biodegradability of chitosan/sodium alginate hydrogels, along with their demonstrated polymerization and disintegration characteristics in varying pH conditions, have been substantiated by numerous preliminary investigations.

Consequently, chitosan/sodium alginate hydrogels emerge as a rational delivery vehicle for nanoenzyme therapy in colitis. Based on the critical role of ROS in the pathological development of UC and the high antioxidant enzyme activity of Pt NPs, colloidal Pt NPs were synthesized using a reduction method for UC prevention in which PVP acted as a stabilizer and dispersant of metal nanomaterials. First, those with a small particle size were synthesized, and the SOD and CAT liked-activities and hydroxyl radical scavenging ability of the Pt NPs ( $3 \pm 1$  nm) were confirmed using enzyme activity experiments. These antioxidant enzyme activities are the basis for treating UC with Pt NPs.

ROS are pivotal in regulating essential human growth, adaptation, and various physiological processes [66]. An excessive presence of ROS within specific tissues can disturb the delicate equilibrium of oxidation and result in oxidative harm, thereby intensifying the state of chronic inflammation. Macrophages, being immune cells, generate ROS by releasing proinflammatory factors, thereby initiating inflammatory responses [67–69]. Our study assessed Pt NPs' antioxidant capacity using macrophage RAW 264.7 cells as an inflammatory model. The results showed that Pt NPs effectively prevented oxidative stress and protected cells from oxidative damage. In similar experiments, traditional enzymes exhibited lower efficiency in clearing ROS within inflammatory cells than Pt NPs [59]. Moreover, in preventing a UC mouse model, chitosan/alginate hydrogel-loaded Pt NPs significantly reduced various inflammatory markers, indicating the remarkable ability of Pt NPs to ameliorate UC. Histopathological examination of colon smears from the treated group revealed a notable reduction in neutrophil infiltration in colon tissues.

## 5. Conclusions

The colloidal Pt NPs synthesized in this study possessed strong enzymatic activities similar to SOD and CAT, effectively scavenging  $\bullet$ OH radicals. By utilizing chitosan/sodium alginate hydrogels, which possess remarkable biocompatibility and biodegradability, Pt NPs have established a robust basis for effectively eradicating surplus ROS at the inflammatory locus of UC. Pt NPs exhibited remarkable efficacy in mitigating cellular oxidative damage and displaying potent anti-inflammatory properties in models of colitis prevention. Furthermore, Pt NPs did not induce significant systemic toxicity. The findings highlight the considerable potential of Pt NPs as a nanomedicine, providing a novel therapeutic strategy for treating ulcerative colitis.

**Author Contributions:** Conceptualization, H.L. and Y.Z.; methodology, M.Z. (Mingzhen Zhang); writing—original draft preparation, H.L. and Y.Z.; writing—review and editing, Z.Y. and M.Z. (Mingxin Zhang); supervision, M.Z. (Mingzhen Zhang); project administration, Z.Y. and M.Z. (Mingxin Zhang). All authors have read and agreed to the published version of the manuscript.

**Funding:** This research was funded by the National Natural Science Foundation of China, grant number 82000523, the Innovation Team of Xi'an Medical University, grant number 2021TD15, Shaanxi Province Key Research and Development Program, grant number YBSF-072, and the National Science Foundation of Shaanxi, grant number 2023-JC-QN-081.

**Institutional Review Board Statement:** The animal study protocol was approved by the Ethics Committee of Xi'an Jiaotong University (protocol approval n. XJTUAE2023-1564, 13 March 2023).

**Informed Consent Statement:** Not applicable.

**Data Availability Statement:** All the other data supporting the findings of this study are available within the article and from the corresponding author upon reasonable request.

**Acknowledgments:** We thank Xiaofei Wang at the Biomedical Experimental Center of Xi'an Jiaotong University for his assistance with the flow cytometry analysis.

**Conflicts of Interest:** The authors declare no conflict of interest.

## References

1. Gajendran, M.; Loganathan, P.; Jimenez, G.; Catinella, A.P.; Ng, N.; Umopathy, C.; Ziade, N.; Hashash, J.G. A comprehensive review and update on ulcerative colitis. *Dis. Mon.* **2019**, *65*, 100851. [[CrossRef](#)] [[PubMed](#)]
2. Feuerstein, J.D.; Moss, A.C.; Farraye, F.A. Ulcerative Colitis. *Mayo. Clin. Proc.* **2019**, *94*, 1357–1373. [[CrossRef](#)] [[PubMed](#)]
3. Park, J.; Park, S.; Lee, S.A.; Park, S.J.; Cheon, J.H. Improving the care of inflammatory bowel disease (IBD) patients: Perspectives and strategies for IBD center management. *Korean J. Intern. Med.* **2021**, *36*, 1040–1048. [[CrossRef](#)] [[PubMed](#)]
4. Park, J.; Cheon, J.H. Incidence and Prevalence of Inflammatory Bowel Disease across Asia. *Yonsei Med. J.* **2021**, *62*, 99–108. [[CrossRef](#)]
5. Murakami, Y.; Nishiwaki, Y.; Oba, M.S.; Asakura, K.; Ohfuji, S.; Fukushima, W.; Suzuki, Y.; Nakamura, Y. Estimated prevalence of ulcerative colitis and Crohn's disease in Japan in 2014: An analysis of a nationwide survey. *J. Gastroenterol.* **2019**, *54*, 1070–1077. [[CrossRef](#)] [[PubMed](#)]
6. Zeng, Z.; Zhu, Z.; Yang, Y.; Ruan, W.; Peng, X.; Su, Y.; Peng, L.; Chen, J.; Yin, Q.; Zhao, C.; et al. Incidence and clinical characteristics of inflammatory bowel disease in a developed region of Guangdong Province, China: A prospective population-based study. *J. Gastroenterol. Hepatol.* **2013**, *28*, 1148–1153. [[CrossRef](#)]
7. Danese, S.; Sans, M.; Fiocchi, C. Inflammatory bowel disease: The role of environmental factors. *Autoimmun. Rev.* **2004**, *3*, 394–400. [[CrossRef](#)]
8. Hirata, Y.; Ihara, S.; Koike, K. Targeting the complex interactions between microbiota, host epithelial and immune cells in inflammatory bowel disease. *Pharmacol. Res.* **2016**, *113*, 574–584. [[CrossRef](#)]
9. Ferretti, F.; Cannatelli, R.; Monico, M.C.; Maconi, G.; Ardizzone, S. An Update on Current Pharmacotherapeutic Options for the Treatment of Ulcerative Colitis. *J. Clin. Med.* **2022**, *11*, 2302. [[CrossRef](#)]
10. Dai, C.; Huang, Y.H.; Jiang, M. Combination therapy in inflammatory bowel disease: Current evidence and perspectives. *Int. Immunopharmacol.* **2023**, *114*, 109545. [[CrossRef](#)]
11. Mao, R.; Hu, P.J. The Future of IBD Therapy: Where Are We and Where Should We Go Next? *Dig. Dis.* **2016**, *34*, 175–179. [[CrossRef](#)]
12. Liu, X.; Peng, X.; Rong, C.; Zhang, W. Acute pulmonary embolism following corticosteroid administration in acute severe ulcerative colitis with gastrointestinal bleeding: A case report. *Front. Cardiovasc. Med.* **2022**, *9*, 1018462. [[CrossRef](#)]
13. Eriksson, C.; Rundquist, S.; Cao, Y.; Montgomery, S.; Halfvarson, J. Impact of thiopurines on the natural history and surgical outcome of ulcerative colitis: A cohort study. *Gut* **2019**, *68*, 623–632. [[CrossRef](#)] [[PubMed](#)]
14. Tian, T.; Wang, Z.; Zhang, J. Pathomechanisms of Oxidative Stress in Inflammatory Bowel Disease and Potential Antioxidant Therapies. *Oxid. Med. Cell Longev.* **2017**, *2017*, 4535194. [[CrossRef](#)] [[PubMed](#)]
15. Piechota-Polanczyk, A.; Fichna, J. Review article: The role of oxidative stress in pathogenesis and treatment of inflammatory bowel diseases. *Naunyn. Schmiedebergs Arch. Pharm.* **2014**, *387*, 605–620. [[CrossRef](#)]
16. Pereira, C.; Grácio, D.; Teixeira, J.P.; Magro, F. Oxidative Stress and DNA Damage: Implications in Inflammatory Bowel Disease. *Inflamm. Bowel. Dis.* **2015**, *21*, 2403–2417. [[CrossRef](#)] [[PubMed](#)]
17. Guan, G.; Lan, S. Implications of Antioxidant Systems in Inflammatory Bowel Disease. *Biomed. Res. Int.* **2018**, *2018*, 1290179. [[CrossRef](#)] [[PubMed](#)]
18. Zhao, H.; Zhang, R.; Yan, X.; Fan, K. Superoxide dismutase nanozymes: An emerging star for anti-oxidation. *J. Mater. Chem. B* **2021**, *9*, 6939–6957. [[CrossRef](#)]
19. Carocho, M.; Ferreira, I.C. A review on antioxidants, prooxidants and related controversy: Natural and synthetic compounds, screening and analysis methodologies and future perspectives. *Food Chem. Toxicol.* **2013**, *51*, 15–25. [[CrossRef](#)]
20. Zhao, T.; Wu, W.; Sui, L.; Huang, Q.; Nan, Y.; Liu, J.; Ai, K. Reactive oxygen species-based nanomaterials for the treatment of myocardial ischemia reperfusion injuries. *Bioact. Mater.* **2022**, *7*, 47–72. [[CrossRef](#)]

21. Yu, Z.; Lou, R.; Pan, W.; Li, N.; Tang, B. Nanoenzymes in disease diagnosis and therapy. *Chem. Commun.* **2020**, *56*, 15513–15524. [[CrossRef](#)] [[PubMed](#)]
22. Narayanan, R.; El-Sayed, M.A. Shape-Dependent Catalytic Activity of Platinum Nanoparticles in Colloidal Solution. *Nano Lett.* **2004**, *4*, 1343–1348. [[CrossRef](#)]
23. Katsumi, H.; Fukui, K.; Sato, K.; Maruyama, S.; Yamashita, S.; Mizumoto, E.; Kusamori, K.; Oyama, M.; Sano, M.; Sakane, T.; et al. Pharmacokinetics and preventive effects of platinum nanoparticles as reactive oxygen species scavengers on hepatic ischemia/reperfusion injury in mice. *Metallomics* **2014**, *6*, 1050–1056. [[CrossRef](#)] [[PubMed](#)]
24. Zheng, W.; Jiang, B.; Hao, Y.; Zhao, Y.; Zhang, W.; Jiang, X. Screening reactive oxygen species scavenging properties of platinum nanoparticles on a microfluidic chip. *Biofabrication* **2014**, *6*, 045004. [[CrossRef](#)]
25. Koczkur, K.M.; Mourdikoudis, S.; Polavarapu, L.; Skrabalak, S.E. Polyvinylpyrrolidone (PVP) in nanoparticle synthesis. *Dalton Trans.* **2015**, *44*, 17883–17905. [[CrossRef](#)]
26. Chen, X.; Fan, M.; Tan, H.; Ren, B.; Yuan, G.; Jia, Y.; Li, J.; Xiong, D.; Xing, X.; Niu, X.; et al. Magnetic and self-healing chitosan-alginate hydrogel encapsulated gelatin microspheres via covalent cross-linking for drug delivery. *Mater. Sci. Eng. C Mater. Biol. Appl.* **2019**, *101*, 619–629. [[CrossRef](#)]
27. Yang, M.; Yang, C.; Zhang, Y.; Yan, X.; Ma, Y.; Zhang, Y.; Cao, Y.; Xu, Q.; Tu, K.; Zhang, M. An oral pH-activated "nano-bomb" carrier combined with berberine by regulating gene silencing and gut microbiota for site-specific treatment of ulcerative colitis. *Biomater. Sci.* **2022**, *10*, 1053–1067. [[CrossRef](#)]
28. Kim, Y.; Zharkinbekov, Z.; Raziyeva, K.; Tabyldiyeva, L.; Berikova, K.; Zhumagul, D.; Temirkhanova, K.; Saparov, A. Chitosan-Based Biomaterials for Tissue Regeneration. *Pharmaceutics* **2023**, *15*, 807. [[CrossRef](#)]
29. Wei, W.; Zhang, Y.; Li, R.; Cao, Y.; Yan, X.; Ma, Y.; Zhang, Y.; Yang, M.; Zhang, M. Oral Delivery of Pterostilbene by L-Arginine-Mediated "Nano-Bomb" Carrier for the Treatment of Ulcerative Colitis. *Int. J. Nanomed.* **2022**, *17*, 603–616. [[CrossRef](#)]
30. Xiao, B.; Zhang, Z.; Viennois, E.; Kang, Y.; Zhang, M.; Han, M.K.; Chen, J.; Merlin, D. Combination Therapy for Ulcerative Colitis: Orally Targeted Nanoparticles Prevent Mucosal Damage and Relieve Inflammation. *Theranostics* **2016**, *6*, 2250–2266. [[CrossRef](#)]
31. Xiao, B.; Viennois, E.; Chen, Q.; Wang, L.; Han, M.K.; Zhang, Y.; Zhang, Z.; Kang, Y.; Wan, Y.; Merlin, D. Silencing of Intestinal Glycoprotein CD98 by Orally Targeted Nanoparticles Enhances Chemosensitization of Colon Cancer. *ACS Nano* **2018**, *12*, 5253–5265. [[CrossRef](#)] [[PubMed](#)]
32. Zhang, Y.; Zhao, J.; Zhang, L.; Zhao, Y.; Zhang, Y.; Cheng, L.; Wang, D.; Liu, C.; Zhang, M.; Fan, K.; et al. A cascade nanoreactor for enhancing sonodynamic therapy on colorectal cancer via synergistic ROS augment and autophagy blockage. *Nano Today* **2023**, *49*, 101798. [[CrossRef](#)]
33. Fornaguera, C.; Solans, C. Characterization of Polymeric Nanoparticle Dispersions for Biomedical Applications: Size, Surface Charge and Stability. *Pharm. Nanotechnol.* **2018**, *6*, 147–164. [[CrossRef](#)] [[PubMed](#)]
34. Aragón, F.H.; Coaquira, J.A.; Villegas-Lelovsky, L.; da Silva, S.W.; Cesar, D.F.; Nagamine, L.C.; Cohen, R.; Menéndez-Proupin, E.; Morais, P.C. Evolution of the doping regimes in the Al-doped SnO<sub>2</sub> nanoparticles prepared by a polymer precursor method. *J. Phys. Condens. Matter* **2015**, *27*, 095301. [[CrossRef](#)]
35. Choi, H.J.; Kim, S.; Chu, E.K.; Noh, B.R.; Lee, W.S.; Kwon, S.H.; Oh, S.; Kim, K.K. Enhanced Photon Emission Efficiency Using Surface Plasmon Effect of Pt Nanoparticles in Ultra-Violet Emitter. *Micromachines* **2019**, *10*, 528. [[CrossRef](#)]
36. Lu, Y.; Wang, D.; Mou, Z.; Huang, J.; Du, Y.; Yang, P. Triphenylamine-based dye functionalized platinum colloid for photocatalytic hydrogen evolution from water: Synthesis, characterization, electron transfer, and photocatalysis. *Colloids Surf. A Physicochem. Eng. Asp.* **2014**, *457*, 282–287. [[CrossRef](#)]
37. Teow, Y.; Valiyaveetil, S. Active targeting of cancer cells using folic acid-conjugated platinum nanoparticles. *Nanoscale* **2010**, *2*, 2607–2613. [[CrossRef](#)]
38. Zhao, J.; Gao, W.; Cai, X.; Xu, J.; Zou, D.; Li, Z.; Hu, B.; Zheng, Y. Nanozyme-mediated catalytic nanotherapy for inflammatory bowel disease. *Theranostics* **2019**, *9*, 2843–2855. [[CrossRef](#)]
39. Jain, A.K.; Thareja, S. In vitro and in vivo characterization of pharmaceutical nanocarriers used for drug delivery. *Artif. Cells Nanomed. Biotechnol.* **2019**, *47*, 524–539. [[CrossRef](#)]
40. Halliwell, B.; Adhikary, A.; Dingfelder, M.; Dizdaroglu, M. Hydroxyl radical is a significant player in oxidative DNA damage in vivo. *Chem. Soc. Rev.* **2021**, *50*, 8355–8360. [[CrossRef](#)]
41. Balmus, I.M.; Ciobica, A.; Trifan, A.; Stanciu, C. The implications of oxidative stress and antioxidant therapies in Inflammatory Bowel Disease: Clinical aspects and animal models. *Saudi J. Gastroenterol.* **2016**, *22*, 3–17. [[CrossRef](#)]
42. Secondo, L.E.; Avrutin, V.; Ozgur, U.; Topsakal, E.; Lewinski, N.A. Real-time monitoring of cellular oxidative stress during aerosol sampling: A proof of concept study. *Drug Chem. Toxicol.* **2022**, *45*, 767–774. [[CrossRef](#)]
43. Kunzmann, A.; Andersson, B.; Thurnherr, T.; Krug, H.; Scheynius, A.; Fadeel, B. Toxicology of engineered nanomaterials: Focus on biocompatibility, biodistribution and biodegradation. *Biochim. Biophys. Acta* **2011**, *1810*, 361–373. [[CrossRef](#)]
44. Zor, F.; Selek, F.N.; Orlando, G.; Williams, D.F. Biocompatibility in regenerative nanomedicine. *Nanomedicine (Lond)* **2019**, *14*, 2763–2775. [[CrossRef](#)] [[PubMed](#)]
45. Li, D.F.; Yang, M.F.; Xu, H.M.; Zhu, M.Z.; Zhang, Y.; Tian, C.M.; Nie, Y.Q.; Wang, J.Y.; Liang, Y.J.; Yao, J.; et al. Nanoparticles for oral delivery: Targeted therapy for inflammatory bowel disease. *J. Mater Chem. B* **2022**, *10*, 5853–5872. [[CrossRef](#)] [[PubMed](#)]
46. Liu, R.; Gan, J.; Du, M.; Kong, X.; Xu, C.; Lü, Y.; Cao, S.; Meng, T.; Wang, B.; Yu, T. Preparation and Characterization of Multilayer pH-Responsive Hydrogel Loaded Ganoderma lucidum Peptides. *Foods* **2023**, *12*, 1481. [[CrossRef](#)] [[PubMed](#)]

47. Chen, K.H.; Lundy, D.J.; Toh, E.K.; Chen, C.H.; Shih, C.; Chen, P.; Chang, H.C.; Lai, J.J.; Stayton, P.S.; Hoffman, A.S.; et al. Nanoparticle distribution during systemic inflammation is size-dependent and organ-specific. *Nanoscale* **2015**, *7*, 15863–15872. [[CrossRef](#)] [[PubMed](#)]
48. Bronte, V.; Pittet, M.J. The spleen in local and systemic regulation of immunity. *Immunity* **2013**, *39*, 806–818. [[CrossRef](#)] [[PubMed](#)]
49. Harold, K.M.; MacCuaig, W.M.; Holter-Charkabarty, J.; Williams, K.; Hill, K.; Arreola, A.X.; Sekhri, M.; Carter, S.; Gomez-Gutierrez, J.; Salem, G.; et al. Advances in Imaging of Inflammation, Fibrosis, and Cancer in the Gastrointestinal Tract. *Int. J. Mol. Sci.* **2022**, *23*, 16109. [[CrossRef](#)] [[PubMed](#)]
50. Kaenkumchorn, T.; Wahbeh, G. Ulcerative Colitis: Making the Diagnosis. *Gastroenterol. Clin. N. Am.* **2020**, *49*, 655–669. [[CrossRef](#)] [[PubMed](#)]
51. Ramos, L.; Teo-Loy, J.; Barreiro-de Acosta, M. Disease clearance in ulcerative colitis: Setting the therapeutic goals for future in the treatment of ulcerative colitis. *Front. Med.* **2022**, *9*, 1102420. [[CrossRef](#)]
52. Choi, C.H.; Rutter, M.D.; Askari, A.; Lee, G.H.; Warusavitarne, J.; Moorghen, M.; Thomas-Gibson, S.; Saunders, B.P.; Graham, T.A.; Hart, A.L. Forty-Year Analysis of Colonoscopic Surveillance Program for Neoplasia in Ulcerative Colitis: An Updated Overview. *Am. J. Gastroenterol.* **2015**, *110*, 1022–1034. [[CrossRef](#)] [[PubMed](#)]
53. Yashiro, M. Ulcerative colitis-associated colorectal cancer. *World J. Gastroenterol.* **2014**, *20*, 16389–16397. [[CrossRef](#)] [[PubMed](#)]
54. Krugliak Cleveland, N.; Torres, J.; Rubin, D.T. What Does Disease Progression Look Like in Ulcerative Colitis, and How Might It Be Prevented? *Gastroenterology* **2022**, *162*, 1396–1408. [[CrossRef](#)]
55. Hibiya, S.; Matsuyama, Y.; Fujii, T.; Maeyashiki, C.; Saito, E.; Ito, K.; Shimizu, H.; Kawamoto, A.; Motobayashi, M.; Takenaka, K.; et al. 5-aminosalicylate-intolerant patients are at increased risk of colectomy for ulcerative colitis. *Aliment. Pharm.* **2021**, *53*, 103–113. [[CrossRef](#)]
56. Kałużna, A.; Olczyk, P.; Komosińska-Vassev, K. The Role of Innate and Adaptive Immune Cells in the Pathogenesis and Development of the Inflammatory Response in Ulcerative Colitis. *J. Clin. Med.* **2022**, *11*, 400. [[CrossRef](#)]
57. Zhang, R.; Fan, K.; Yan, X. Nanozymes: Created by learning from nature. *Sci. China Life Sci.* **2020**, *63*, 1183–1200. [[CrossRef](#)]
58. Sheng, Y.; Li, H.L.; Liu, M.J.; Xie, B.X.; Wei, W.; Wu, J.W.; Meng, F.G.; Wang, H.Y.; Chen, S. A Manganese-Superoxide Dismutase From *Thermus thermophilus* HB27 Suppresses Inflammatory Responses and Alleviates Experimentally Induced Colitis. *Inflamm. Bowel. Dis.* **2019**, *25*, 1644–1655. [[CrossRef](#)]
59. Zou, Q.; Feng, J.; Li, T.; Cheng, G.; Wang, W.; Rao, G.; He, H.; Li, Y. Antioxidation and anti-inflammatory actions of the extract of *Nitraria Tangutorum* Bobr. fruits reduce the severity of ulcerative colitis in a dextran sulphate sodium-induced mice model. *J. Funct. Foods* **2022**, *91*, 105005. [[CrossRef](#)]
60. Huang, Y.; Jiang, J.; Wang, Y.; Chen, J.; Xi, J. Nanozymes as Enzyme Inhibitors. *Int. J. Nanomed.* **2021**, *16*, 1143–1155. [[CrossRef](#)]
61. Zhang, B.; Lv, Y.; Yu, C.; Zhang, W.; Song, S.; Li, Y.; Chong, Y.; Huang, J.; Zhang, Z. Au-Pt nanozyme-based multifunctional hydrogel dressing for diabetic wound healing. *Biomater. Adv.* **2022**, *137*, 212869. [[CrossRef](#)] [[PubMed](#)]
62. Moglianetti, M.; De Luca, E.; Pedone, D.; Marotta, R.; Catelani, T.; Sartori, B.; Amenitsch, H.; Retta, S.F.; Pompa, P.P. Platinum nanozymes recover cellular ROS homeostasis in an oxidative stress-mediated disease model. *Nanoscale* **2016**, *8*, 3739–3752. [[CrossRef](#)] [[PubMed](#)]
63. Elmazoglu, Z.; Kayhan, H.; Santamaría, A.; Rangel-López, E.; Uğur, P.K.; Ceylan, A.; Aschner, M.; Karasu, Ç. Platinum nanoparticles Protect Against Lipopolysaccharide-Induced Inflammation in Microglial BV-2 Cells via Decreased Oxidative Damage and Increased Phagocytosis. *Neurochem. Res.* **2021**, *46*, 3325–3341. [[CrossRef](#)]
64. Li, C.; Obireddy, S.R.; Lai, W.F. Preparation and use of nanogels as carriers of drugs. *Drug Deliv.* **2021**, *28*, 1594–1602. [[CrossRef](#)] [[PubMed](#)]
65. Jiang, Y.; Chen, J.; Deng, C.; Suuronen, E.J.; Zhong, Z. Click hydrogels, microgels and nanogels: Emerging platforms for drug delivery and tissue engineering. *Biomaterials* **2014**, *35*, 4969–4985. [[CrossRef](#)] [[PubMed](#)]
66. Yang, B.; Chen, Y.; Shi, J. Reactive Oxygen Species (ROS)-Based Nanomedicine. *Chem. Rev.* **2019**, *119*, 4881–4985. [[CrossRef](#)]
67. Rendra, E.; Riabov, V.; Mossel, D.M.; Sevastyanova, T.; Harmsen, M.C.; Kzhyshkowska, J. Reactive oxygen species (ROS) in macrophage activation and function in diabetes. *Immunobiology* **2019**, *224*, 242–253. [[CrossRef](#)]
68. Geiß, C.; Salas, E.; Guevara-Coto, J.; Régnier-Vigouroux, A.; Mora-Rodríguez, R.A. Multistability in Macrophage Activation Pathways and Metabolic Implications. *Cells* **2022**, *11*, 404. [[CrossRef](#)]
69. Yang, Z.; Min, Z.; Yu, B. Reactive oxygen species and immune regulation. *Int. Rev. Immunol.* **2020**, *39*, 292–298. [[CrossRef](#)]

**Disclaimer/Publisher’s Note:** The statements, opinions and data contained in all publications are solely those of the individual author(s) and contributor(s) and not of MDPI and/or the editor(s). MDPI and/or the editor(s) disclaim responsibility for any injury to people or property resulting from any ideas, methods, instructions or products referred to in the content.